An Initial Report on the Performance of Post Contrast Self-Navigated Whole-Heart Coronary MRI in Patients with Suspected or Established Coronary Artery Disease

Davide Piccini[1,2], Christophe Sierro[3], Juerg Schwitter[3], Pierre Monney[3], Gabriella Vincenti[3], Simon C. Koestner[3], Didier Locca[3], Tobias Rutz[3], Arne Littmann[4], Michael O. Zenge[4], Gunnar Krueger[1,5], and Matthias Stuber[2]

[1]Advanced Clinical Imaging Technology, Siemens Healthcare IM S AW, Lausanne, Switzerland, [2]Department of Radiology, University Hospital (CHUV) and University of Lausanne (UNIL) / Center for Biomedical Imaging (CIBM), Lausanne, Switzerland, [3]Division of Cardiology and Cardiac MR Center, University Hospital of Lausanne (CHUV), Lausanne, Switzerland, [4]MR Application and Workflow Development, Healthcare Sector, Siemens AG, Erlangen, Germany, [5]CIBM-AIT, Ecole Polytechnique Federale de Lausanne, Lausanne, Switzerland

INTRODUCTION: Whole-heart MR imaging with high isotropic spatial resolution has shown to be a valuable tool to easily assess information on both cardiac and coronary anatomy in one single scan. Although such acquisition eliminates the need of a pre-localization of the coronary arteries, the large amount of acquired data mandates that the examination be performed during free-breathing. Contemporary navigator gated and corrected approaches assume a linear relationship between respiratory-induced heart and liver displacement together with a constant tracking factor [1]. However, in practice, this relationship is not always linear, tracking factors are individually dependent, and hysteresis between respiratory induced heart and liver motion has been reported [2]. This may contribute to variable image quality particulary in patients with irregular breathing. Related to that, such approaches still suffer from limited and unpredictable navigator efficiency [3]. Conversely, self-navigation (SN) [4] allows for respiratory motion correction without navigators, as the motion estimation is directly extracted from image data acquired at the level of the heart, thus avoiding many of these disadvantages. In particular, SN enables simplified examination planning, an improved accuracy of the motion compensation and a priori knowledge of the acquisition duration, as 100% acceptance rate is achieved [4,5] regardless of the individual respiratory pattern. While SN whole heart human data have successfully been acquired in healthy adult subjects, the performance of this technique remains to be ascertained in patients with suspected or established coronary artery disease. For these reasons, our 3D SN whole-heart technique [5] was integrated as an optional component in clinical examinations, where the time gap between perfusion imaging and 2D late gadolinium enhancement (2D-LGE) was exploited. The aim of this work was to evaluate the image quality and diagnostic performance of the SN acquisitions for the detection of coronary artery stenoses as well as for the identification of congenital anomalies of the coronary arteries.

METHODS: In this preliminary study, whole-heart 3D SN datasets were acquired in a total of 60 patients (35 men, mean age 47.7±20.6 y), as an adjunct to routine clinical examinations. All the acquisitions were performed on a 1.5T clinical MRI scanner (MAGNETOM Aera, Siemens AG, Healthcare Sector, Erlangen, Germany). A total of 24 elements of the anterior and posterior phased-array coils were activated for signal reception. Data acquisition was performed with a 3D radial trajectory implementing the spiral phyllotaxis pattern [6], adapted to self-navigation as described in [5]. All measurements were segmented and ECG-triggered. A T_2-preparation pulse was added before each segment to the fat-saturated bSSFP imaging sequence. The 3D SN acquisition started approximately 4 min after injection of a bolus of 2 mmol/kg of Gadobutrol (Gadovist, Bayer Schering Pharma, Zurich, Switzerland). Imaging was performed with the following parameters: TR/TE 3.1/1.56 ms, FOV $(220mm)^3$, matrix 192^3, acquired voxel size $(1.15mm)^3$, radio frequency (RF) excitation angle 115°, and receiver bandwidth 900 Hz/Pixel. A total of 12000 radial readouts were acquired either in 377 (acquisition window (AW) = 100ms) or 610 (AW = 75ms) heartbeats, depending on the heart rate of the subject and with overall sampling ratio of 20%, with respect to the Nyquist limit. The trigger delay was set using visual inspection of the most quiescent mid-diastolic period on a mid-ventricular short axis cine image series acquired prior to the injection of the contrast agent. The proximal, mid and distal segments of the right coronary artery (RCA), and of the left anterior descending artery (LAD), the left main stem (LM) and the proximal segment of the left circumflex artery (LCX) were graded for image quality by two experts (M.S. and D.P.) according to [7]. Any segment with grade >0 was considered as "visualized". Vessel length was computed for all coronary arteries. Where x-ray angiograms were available (18 cases), a double-blinded evaluation for the detection of coronary stenoses was performed. The stenoses on the x-ray angiograms were identified by an experienced clinician (C.S.), while the MRA reading was performed by M.S. and D.P. Sensitivity and specificity were computed for the proximal and mid segments of the RCA and of the LAD. The duration of all SN acquisitions was recorded. The performance of the SN technique was also tested for visualization of congenital malformations of the coronary arteries in 6 patients.

RESULTS: The average acquisition time for the SN protocol was 6.5±1.9 min. Average vessel length, "visualization" rates, and average image quality grades for all coronary segments are reported in Table 1. The quality grades of LM, prox. LAD and prox. and mid RCA were significantly higher than those from all the distal segments, even after Bonferroni correction (p<0.001). The double blinded comparison with x-ray angiography (Fig. 1) resulted in sensitivity and specificity of 67.8% and 80.0% on a total of 72 coronary segments. Anomalous origin and course of the coronary arteries could be visualized in all congenital cases (Fig. 2).

DISCUSSION AND CONCLUSIONS: This preliminary patient study demonstrates that post-contrast 3D SN whole-heart coronary MRA with high isotropic spatial resolution is feasible and can optionally be integrated into routine clinical scans. A good visualization of the proximal to mid segments of the coronary arteries is routinely obtained and congenital malformations can be visualized. However, the average image quality as well as the spatial and temporal resolution (i.e. the acquisition window) remains to be improved to further advance diagnostic quality for the assessment of proximal and mid luminal coronary artery disease.

REFERENCES: [1] Wang Y, et al MRM 1995; 33:713-719; [2] Nehrke K, et al, Radiology 2001; 220:810-815; [3] Stuber M, et al, Radiology 1999; 212:579-587; [4] Stehning C, et al, MRM 2005; 54:476-480; [5] Piccini D, et al, MRM 2012; 68:571-579; [6] Piccini D, et al, MRM 2011; 66:1049-1056; [7] McConnell MV, et al, AJR 1997; 168:1369-1375.
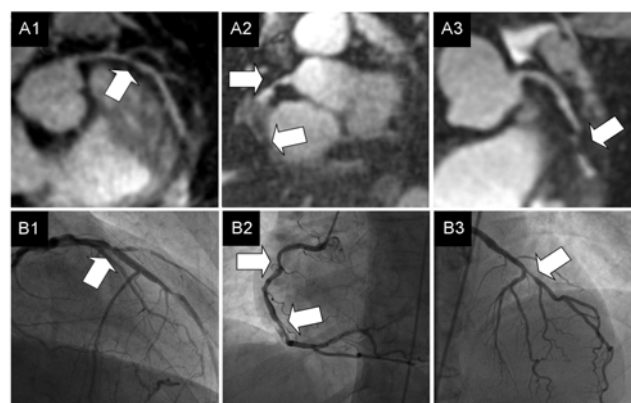
Figure 1: Example comparing multiplanar reformats of the whole-heart SN coronary MRI datasets (top row, A) with the correspondent x-ray coronary angiograms (bottom row, B): stenosis of the mid LAD (1), inter-stent re-stenoses of the proximal RCA between two stents (2) (the bright artifact between the two stenoses in A2 is caused by the stent), and another stenosis of the mid LAD (3).

	LM	LAD:	Prox	Mid	Dist
Length [mm]:	16.0 ± 5.4	64.8 ± 36.1			
Visualized:	59 / 60		55 / 60	49 / 60	39 / 60
Grade:	2.1 ± 1.0		1.8±1.1	1.3±1.0	0.8 ± 0.8

	LCX:	Prox	RCA:	Prox	Mid	Dist
Length [mm]:	25.8 ± 23.1		77.4 ± 44.2			
Visualized:		48 / 60		58 / 60	55 / 60	33 / 60
Grade:		1.2 ± 0.9		2.0 ± 01.0	1.6 ± 1.0	0.6 ± 0.7

Table 1: Results of the quantitative analysis on the 60 patient datasets
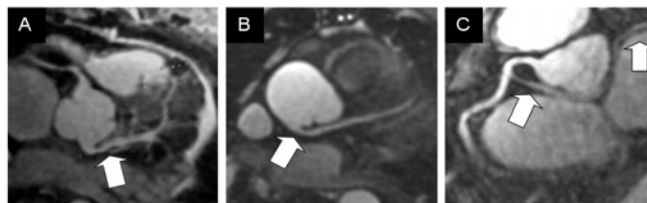

Figure 2: Examples of anomalous coronary arteries imaged with the SN sequence: surgically reconstructed LM stem in a case of abnormal left coronary artery arising from the pulmonary artery (ALCAPA syndrome) (A), abnormal LM arising from the non-coronary sinus and running between the aorta and the left atrium (B) anomalous origin and course of the LCX originating from the proximal RCA (C).